Clinical Cancer Research

Potential Mechanisms for Thrombocytopenia Development with Trastuzumab Emtansine (T-DM1)

Hirdesh Uppal[1], Estelle Doudement[1], Kaushiki Mahapatra[1], Walter C. Darbonne[2], Daniela Bumbaca[3], Ben-Quan Shen[3], Xiaoyan Du[2], Ola Saad[4], Kristin Bowles[5], Steve Olsen[6], Gail D. Lewis Phillips[7], Dylan Hartley[1], Mark X. Sliwkowski[7], Sandhya Girish[8], Donna Dambach[9], and Vanitha Ramakrishnan[10]

Abstract

Purpose: Trastuzumab-emtansine (T-DM1) is an antibody–drug conjugate (ADC) comprising the cytotoxic agent DM1 conjugated to trastuzumab with a stable linker. Thrombocytopenia was the dose-limiting toxicity in the phase I study, and grade $\geq$3 thrombocytopenia occurred in up to 13% of patients receiving T-DM1 in phase III studies. We investigated the mechanism of T-DM1–induced thrombocytopenia.

Experimental Design: The effect of T-DM1 on platelet function was measured by aggregometry, and by flow cytometry to detect the markers of activation. The effect of T-DM1 on differentiation and maturation of megakaryocytes (MK) from human hematopoietic stem cells was assessed by flow cytometry and microscopy. Binding, uptake, and catabolism of T-DM1 in MKs, were assessed by various techniques including fluorescence microscopy, scintigraphy to detect T-[H^3]-DM1 and ^{125}I-T-DM1, and mass spectrometry. The role of FcγRIIa was assessed using blocking antibodies and mutant constructs of trastuzumab that do not bind FcγR.

Results: T-DM1 had no direct effect on platelet activation and aggregation, but it did markedly inhibit MK differentiation via a cytotoxic effect. Inhibition occurred with DM1-containing ADCs but not with trastuzumab demonstrating a role for DM1. MKs internalized these ADCs in a HER2-independent, FcγRIIa-dependent manner, resulting in intracellular release of DM1. Binding and internalization of T-DM1 diminished as MKs matured; however, prolonged exposure of mature MKs to T-DM1 resulted in a disrupted cytoskeletal structure.

Conclusions: These data support the hypothesis that T-DM1–induced thrombocytopenia is mediated in large part by DM1-induced impairment of MK differentiation, with a less pronounced effect on mature MKs. *Clin Cancer Res; 21(1); 123–33.* *©2014 AACR.*

Introduction

One of the major limitations of systemic chemotherapy for cancer is the development of dose-limiting toxicity, caused by the exposure of nontumor cells to cytotoxic agents. Antibody–drug conjugates (ADC) are composed of a cytotoxic agent conjugated to a targeted antibody via a covalent linker (1). ADCs are designed to deliver this cytotoxic agent selectively to tumor cells, thereby minimizing systemic toxicity.

Trastuzumab-emtansine (T-DM1) is an ADC comprising the cytotoxic agent DM1 conjugated via a stable thioether linker to the humanized human EGFR2 (HER2)-targeted monoclonal antibody trastuzumab (2). T-DM1 binds to HER2 with an affinity similar to that of unconjugated trastuzumab (3). T-DM1 is internalized, and the active catabolite lysine-N^{ε}- maleimidomethyl]-cyclohexane-1-carboxylate (MCC)-DM1 is released by lysosomal degradation (4), resulting in microtubule destabilization and subsequent inhibition of cell division and proliferation of HER2-positive cancer cells (2, 3). Like trastuzumab, T-DM1 binding to cell surface HER2 results in antitumor activities—including mediation of antibody-dependent cellular cytotoxicity, inhibition of proliferative signaling through the PI3K/serine/threonine kinase (Akt) pathway, and inhibition of proteolytic cleavage of the extracellular domain of HER2—preventing shedding of HER2 into the circulation (3).

[1]Department of Safety Assessment, Genentech, Inc, South San Francisco, California. [2]Department of Oncology Biomarker Development, Development Sciences, gRED, Genentech, Inc, South San Francisco, California. [3]Department of Preclinical and Translational Pharmacokinetics and Pharmodynamics, Genentech, Inc, South San Francisco, California. [4]Department of Bioanalytical Sciences, Genentech, Inc, South San Francisco, California. [5]Department of Protein Chemistry, Genentech, Inc, South San Francisco, California. [6]Department of Product Development, Genentech, Inc, South San Francisco, California. [7]Department of Molecular Oncology, Genentech, Inc, South San Francisco, California. [8]Department of Development Sciences, Genentech, Inc, South San Francisco, California. [9]Department of Small Molecule and Investigative Toxicology, Genentech, Inc, South San Francisco, California. [10]Department of Project Management and Operations, Genentech, Inc, South San Francisco, California.

Note: Supplementary data for this article are available at Clinical Cancer Research Online (http://clincancerres.aacrjournals.org/).

Current address for H. Uppal: Department of Diagnostics, Medivation, San Francisco, CA; current address for X. Du, Department of Biologics Operations, Merck Research Laboratories, Palo Alto, CA; current address for S. Olsen, Department of Global Medical Affairs-Oncology, Astra Zeneca PLC, London, United Kingdom; and Current address for D. Hartley, Department of Drug Metabolism and Pharmacokinetics, Array Biopharma, Inc., Boulder, CO.

Corresponding Author: Vanitha Ramakrishnan, Project Management and Operations, 1 DNA Way, South San Francisco, CA 94080. Phone: 650-467-3912; Fax: 650-467-5476; E-mail: vanithar@gene.com

doi: 10.1158/1078-0432.CCR-14-2093

Translational Relevance

These experiments may impact patient care by increasing our understanding of mechanisms of trastuzumab-emtansine (T-DM1)-induced thrombocytopenia. T-DM1 is an antibody–drug conjugate recently approved for treatment of HER2-positive metastatic breast cancer. Thrombocytopenia was the dose-limiting toxicity in the phase I study, and the most commonly reported grade ≥3 adverse event in phase III studies. We investigated the effect of T-DM1 on human platelets and megakaryocytes *ex vivo*. Here, we show that T-DM1 had no direct effect on platelet activation and aggregation. T-DM1 did, however, inhibit megakaryocyte differentiation from hematopoietic stem cells. This effect appears to be mediated by DM1, which was internalized by megakaryocytes in a HER2-independent, FcγRIIa-dependent manner. Our data support the hypothesis that impaired platelet production by megakaryocytes mediates much of the thrombocytopenia observed in clinical trials, and underscore the need to evaluate the role of Fcγ receptors in toxicities seen with antibody therapeutics on nontarget cells.

T-DM1 is approved for the treatment of patients with previously treated metastatic breast cancer. T-DM1 has been generally well tolerated with a lower incidence of grade ≥3 adverse events compared with trastuzumab plus docetaxel (46.4% vs. 90.9%; ref. 5) and lapatinib plus capecitabine (40.8% vs. 57.0%; ref. 6). Thrombocytopenia was the dose-limiting toxicity with T-DM1 (7) and grade ≥3 thrombocytopenia was observed in 4.7% (8) to 12.9% (6) of patients in phase III studies. In most patients who receive T-DM1 once every 21 days, concentrations of circulating platelets show a pattern of cyclic decline, often below the normal range, followed by recovery to normal before the next dose (6, 7, 9, 10). Although the predose platelet count remains consistent for the duration of the treatment course in many patients, others exhibit a slow downward drift in predose platelet counts with repeated cycles of T-DM1 (10). Other hematologic lineages appear to be relatively unaffected by T-DM1, with low rates of severe anemia, leukopenia, and neutropenia (5, 6). As with leukocytes and erythrocytes, platelets are not thought to express HER2 (11).

The aim of the current study is to investigate potential mechanisms of T-DM1–induced thrombocytopenia by evaluating the effect of T-DM1 on platelet function and on the differentiation of megakaryocytes (MK) derived *in vitro* from human hematopoietic stem cells (HSC).

Materials and Methods

Platelet isolation

Platelet-rich plasma (PRP) was isolated by low-speed centrifugation of whole blood from normal human donors drawn into trisodium citrate containing bivalirudin and apyrase. For washed platelets (WP), whole blood was obtained from normal human volunteers into acid citrate dextrose. WPs were prepared as described (12) by centrifugation twice in CGS buffer. Platelets were resuspended in Tyrodes-Hepes buffer at 2×10^8/mL for further experiments. For activation experiments, $CaCl_2$ (final concentration 1 mmol/L) was added, and platelets were allowed to rest for 15 minutes at room temperature before use.

Platelet activation

Platelet activation was measured by detecting activated GPIIb/IIIa (i.e., PAC1 binding) and P-selectin (CD62P) expression using flow cytometry. WP (100 μL of 2×10^8/mL) or PRP was aliquoted into 96-well conical well plates and activated at 4°C for 10 minutes using collagen (1 to 10 μg/mL, Chronolog) or TRAP (~1 μmol/L, Sigma-Aldrich) as a positive control, or various test antibodies. Test antibodies included trastuzumab, T-DM1, and the control nonspecific ADC 5B6-DM1 (13). All three test antibodies are of IgG1 isotype. Platelets were diluted 1:1 with ice-cold Tyrodes-Hepes buffer and aliquoted (40 uL aliquots) into triplicate wells containing PE-conjugated anti-CD41 antibody to identify platelets (3 μL) or isotype control and either FITC-conjugated anti-CD62P antibody or FITC-conjugated anti-PAC1 antibody (3 μL) or respective FITC-conjugated isotype controls. Following a 1-hour incubation at 4°C, platelets were diluted and assessed by flow cytometry using a FACSCalibur (BD Biosciences). For experiments assessing the effect of the various test antibodies on agonist-induced activation, WP or PRP was preincubated with the test antibodies for 30 minutes at 4°C and then collagen or TRAP was added for an additional 10-minute incubation.

Platelet aggregation

WP (500 μL, 2×10^8/mL) or PRP (500 μL, ~2×10^8/mL) from normal human donors was pipetted into aggregometer tubes, and aggregation was initiated by the addition of collagen (Chrono-Log; 5 μL of 10 mg/mL solution; 10 μg/mL final concentration) or TRAP (1 μmol/L) as positive controls, or various test antibodies or compounds; and measured in a lumiaggregometer (Chrono-Log 700; Chrono-Log) with stirring (1,000–1,200 rpm) at 37°C. For experiments assessing the effect of the various test antibodies on agonist-induced activation, WP or PRP was preincubated with the test antibodies at 37°C for 30 minutes. Aggregation was initiated with collagen or TRAP and was quantified in a lumiaggregometer.

Differentiation of human MKs

HSCs ($CD133^+/CD34^+$) were purchased from ALLCELLS. Briefly, these HSCs were enriched from bone marrow isolates of healthy donors using positive selection for CD133 and CD34. $CD133^+/CD34^+$ cells were first expanded in cytokine-enriched hematopoietic expansion media (StemSpan CC100; Stem Cell Technologies) for 5 days, then incubated in MK differentiation media [StemSpan CC100 supplemented with thrombopoietin (100 ng/mL), SCF (25 ng/mL), IL3 (10 ng/mL), IL6 (10 ng/mL), IL1 (10 ng/mL), and IL9 (10 ng/mL)], for 14 days to obtain multinucleated MKs. Evaluation of the MK differentiation process was performed by flow cytometry, using the MK lineage-specific markers CD41 and CD61 (Supplementary Fig. S1). To obtain mature MKs, day 14 MKs (i.e., immature MKs) were cultured in the same medium for an additional 14 to 16 days (Supplementary Fig. S1B).

MK production and cell viability

Determination of IC_{50}.

To determine the IC_{50} of T-DM1 on immature MKs, $CD133^+/CD34^+$ cells were resuspended in MK differentiation medium (750,000 cells/well) and treated with different concentrations of T-DM1, trastuzumab, 5B6-DM1, or vehicle (100 μg/mL, 25 μg/mL, 6.25 μg/mL, 1.56 μg/mL, 0.39 μg/mL, 0.098 μg/mL) for 14 days. At days 3, 6, 9, and 14, three aliquots (25 μL) from each well were evaluated for cellular ATP levels using CellTiter-Glo

luminescence cell viability reagent (Promega). The IC_{50} concentrations were calculated using a four-parameter logistic regression model.

For maturing MKs (day 14 cells), aliquots (100 μL) of cells treated with T-DM1, trastuzumab, or 5B6-DM1 (6.25 μg/mL) at days 17, 20, 23, and 28 postdifferentiation were assessed in triplicate for ATP levels as described above.

On the basis of these experiments, a concentration of 6.25 μg/mL was used for all conjugates and antibodies for subsequent experiments (except where noted).

Flow-cytometric analysis.

$CD133^+/CD34^+$ cells (expanded for 5 days as described earlier) were induced to differentiate for 14 days to obtain immature MKs. Cells in MK differentiation medium were treated with T-DM1, trastuzumab, 5B6-DM1, or vehicle (6.25 μg/mL). At days 3, 6, 9, and 14 of differentiation, the viable cells were counted with an automated cell counter (ViCell, BeckmanCoulter). MK number was determined as follows. An aliquot (500,000 cells per condition) was harvested and washed twice and then incubated for 30 minutes with APC-conjugated mouse anti-human CD41 (BD Pharmingen) and PE-conjugated mouse anti-human CD61 (Miltenyi Biotec Inc.) in the dark at room temperature. Cells were then washed three times with FACs Stain Buffer (FSB; BD Pharmingen) by repeated centrifugation, resuspended in FSB (500 μL), and analyzed by flow cytometry gated for live cells with doublet exclusion and appropriate isotype-matched controls and unstained cells as negative controls. An anti-mouse IgG Compensation Plus bead kit (BD Biosciences) was used for compensation. The MK cell number was calculated as follows for each condition and the percentage of day 0 control was determined:

MK cells per time point = $(\%CD41^+/CD61^+) \times$ # of viable cells in the sample

For ploidy determination, HSCs ($CD133^+/CD34^+$) were expanded for 5 days and differentiated into MKs for 30 days in the presence of antibodies (25 μg/mL). Cells were harvested on selected days during MK differentiation and maturation, washed with cold PBS (0.5 mL), resuspended in FSB (100 μL), and stained for 5 minutes in the dark at room temperature with Hoechst 33342 (1:10,000; Molecular Probes, Life Technologies). The cells were washed three times, resuspended in FSB (500 μL), and analyzed by flow cytometry using Cytobank Flow Cytometer Data Analysis Software (Cytobank, Inc.).

Quantification of catabolites by LC/MS-MS

Catabolite (DM1, MCC-DM1, and Lys-MCC-DM1) concentrations were determined in MK extracts prepared from days 0, 9, and 20. For analysis of MCC-DM1 and Lys-MCC-DM1, an aliquot (30 μL) was extracted by protein precipitation using 80/20 acetonitrile/water (120 μL) containing maytansine (7.5 nmol/L) as an internal standard. To measure DM1, an aliquot (30 μL) of the MK lysates was first treated at 37°C for 15 minutes at pH 6.6 with Tris (2-carboxyethyl)phosphine (1.25 μL, 26 mmol/L; ThermoScientific Pierce) to release any disulfide-bound DM1, and then extracted as described above. The free sulfhydryl on DM1 was blocked by conversion to DM1 N-ethyl maleimide (NEM; 7.9 μL, 25 mmol/L, Sigma-Aldrich) by incubation at 37°C for 45 minutes with NEM.

LC/MS-MS analysis of the extracted samples was conducted using chromatography on a C12 analytical column (Synergi MAX RP 80 A; Phenomenex), followed by TurboIon Spray ionization using an AB SCIEX QTRAP 5500 mass spectrometer. Multiple reaction monitoring scan mode was used for quantification. Transition 845.1/485.1 was monitored for DM1-NEM, 738.2/547.2 for DM1, 975.2/547.5 for MCC-DM1, 1103.2/485.2 for Lys-MCC-DM1, and 692.3/547.4 for maytansine. The DM1-NEM standard curve had a linear range from 0.488 nmol/L to 500.0 nmol/L. The DM1 transition was monitored only to ensure the completion of the NEM derivatization reaction. The MCC-DM1 standard curve had a linear range from 1.953 nmol/L to 500.0 nmol/L, and the Lys-MCC-DM1 standard curve had a linear range from 0.488 nmol/L to 500.0 nmol/L. Data were analyzed using Analyst 1.5.2 software (AB SCIEX).

Binding and internalization of T-DM1 by MKs

Alexa Fluor 488-conjugated trastuzumab and Alexa Fluor 488-conjugated T-DM1 (both at 25 μg/mL) were prepared in the Research Conjugation Lab (Genentech Inc.) by covalent conjugation of Alexa Fluor 488 to proteins via primary amines at a molar fluor-to-antibody ratio of 2:2 and 0.8 for trastuzumab and T-DM1, respectively. MKs (differentiated for 14 days) were preincubated for 10 minutes with or without a blocking anti-CD32 antibody (Miltenyi Biotec). The cells were washed twice with FSB (500 μL) and incubated for 30 minutes in the dark at room temperature with the Alexa Fluor 488-conjugated antibodies (25 μg/mL). The stained cells were plated onto collagen-coated chamber slides (BD Biosciences) and ProLong Gold Antifade Reagent (Life Technologies) was added to the slides before microscopy on an Olympus IX83 motorized inverted fluorescence microscope.

Uptake of radiolabeled antibodies

To assess the contribution of FcγRIIa, the Fc receptor that is expressed on human MKs (14) and platelets (15), to the uptake of T-DM1, we evaluated the uptake of both the parent antibody trastuzumab and a mutant version of trastuzumab (trastuzumab-DANA), in which the Fc region has two mutations, D265A and N297A (16), such that it no longer binds Fcγ receptor. Both forms of trastuzumab were radioiodinated with ^{125}I using Iodogen as previously described (17). [^{125}I]-trastuzumab and [^{125}I]-trastuzumab-DANA antibodies were purified using NAP5TM columns (GE Healthcare Life Sciences) pre-equilibrated in PBS. The specific activities of [^{125}I]-trastuzumab and [^{125}I]-trastuzumab-DANA were 11.0 Ci/g and 10.1 Ci/g, respectively. The radiolabeled antibodies were shown to be intact by size-exclusion HPLC (data not shown). Uptake of these antibodies was used to determine uptake kinetics since ^{125}I-labeled antibodies clear from cells following intracellular antibody degradation.

Both forms of trastuzumab were also conjugated to 1,4,7,10-tetraazacyclododecane-N,N′,N″,N‴-tetraacetic acid (DOTA) and then radiolabeled with $^{111}InCl$ (MDS Nordion; ref. 18). [^{111}In]-trastuzumab and [^{111}In]-trastuzumab-DANA antibodies were purified using NAP5TM columns (GE Healthcare Life Sciences) pre-equilibrated in PBS. The radiolabeled antibodies were shown to be intact by size-exclusion HPLC (data not shown). Uptake of these antibodies was used to determine overall antibody exposure since ^{111}In catabolites accumulate in cells owing to the residualizing properties of the charged and highly polar DOTA chelator.

The uptake and catabolism of labeled antibodies were determined as follows. At day 0, labeled antibodies (1.0 μCi/mL) were added to the cells (4×10^6) at the indicated time points. Cells were harvested and washed three times (0.5 mL each). Incubation

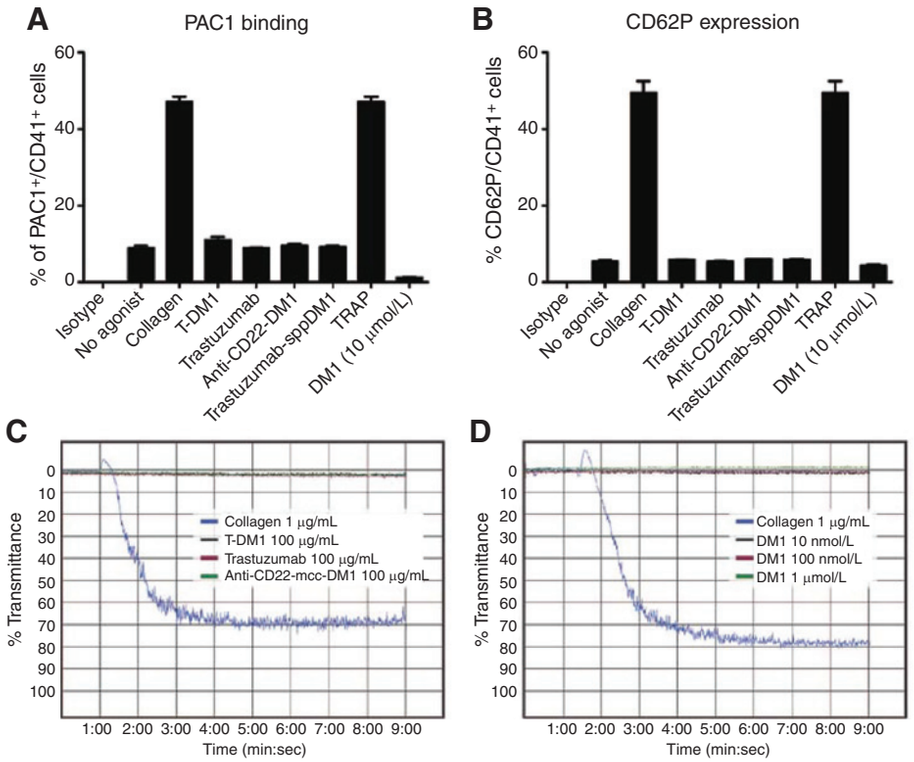

Figure 1.
T-DM1 does not induce activation or aggregation of platelets. Effects of T-DM1, trastuzumab, DM1, and control ADCs (anti-CD22-MCC-DM1, trastuzumab-sppDM1) on *ex vivo* platelet activation in PRP by flow cytometry to measure PAC1 binding (A) and CD62P (P-Selectin; B) expression using collagen and TRAP as positive controls. Isotype-matched controls were used as negative controls for flow cytometry. Representative data with SDs are shown. C, effects of T-DM1, trastuzumab, and a control ADC (anti-CD22-MCC-DM1) on *ex vivo* platelet aggregation in PRP. D, effects of various concentrations of DM1 on *ex vivo* platelet aggregation in PRP. All experiments were conducted in duplicate on platelets from two different donors, and representative data are shown.

media and wash supernatants were collected and used for radioactivity determination. Radioactivity associated with the cell pellet, as well as the media and washes, were quantified by γ-scintigraphy. The percent radioactivity per 10^6 cells for each fraction was determined.

Results

Effect of T-DM1 on platelet activation and aggregation

To determine whether the thrombocytopenia observed in T-DM1–treated patients was caused, at least in part, by a direct effect on mature platelets, we evaluated the effects of T-DM1 and DM1 on the function of platelets isolated from normal donors. Platelets were isolated and utilized either as PRP or WP, as described in the Materials and Methods section, and incubated with T-DM1, DM1, or controls. Neither T-DM1 nor DM1 directly induced platelet activation in PRP, as measured by the expression of activated GPIIb/IIIa (i.e., PAC1 binding; Fig. 1A) and CD62P (Fig. 1B). Expression of these activation markers was similar between resting platelets and platelets treated with T-DM1, trastuzumab, control ADCs, and DM1.

T-DM1 also did not directly induce platelet aggregation in PRP (Fig. 1C) or in WP (Supplementary Fig. S2). To determine whether DM1 induces platelet aggregation, we exposed PRP to DM1 concentrations in the range of those measured in patients treated with T-DM1. On average, maximum systemic plasma DM1 concentrations are 6 ng/mL (8 nmol/L; ref. 19). In PRP, DM1 did not directly induce platelet aggregation at these concentrations (Fig. 1D).

Next, we evaluated the impact of T-DM1 and DM1 on agonist-induced platelet activation and aggregation. Neither T-DM1 nor DM1 had an effect on agonist-induced platelet activation in PRP. Increased PAC1 binding and CD62 expression induced by collagen or TRAP were unaffected by pretreatment with T-DM1, trastuzumab, or control ADC (Fig. 2A and B), or by clinically relevant concentrations of DM1 (Fig. 2C and D). Similarly, neither T-DM1 (Fig. 2E) nor clinically relevant concentrations of DM1 affected agonist-induced platelet aggregation (Fig. 2F). However, at high concentrations (i.e., 100 μmol/L, which is approximately 12,500-fold higher than concentrations measured in patient samples), DM1 inhibited agonist-induced platelet aggregation by 77% (Supplementary Fig. S3).

Effect of T-DM1 on MK differentiation from HSCs

In the absence of a direct, observable effect on platelet activation or aggregation, we evaluated the potential effects of T-DM1 on generation of MKs from HSCs (i.e., $CD133^+/CD34^+$ cells) over time.

Morphology.

On day 9 of differentiation, trastuzumab had no observable effect on MK morphology compared with vehicle control (Supplementary Fig. S4A and S4B). However, treatment with the ADCs T-DM1 or 5B6-DM1 during HSC differentiation altered the cell morphology, inducing a vacuolated morphology consistent with MK death (ref. 20; Supplementary Fig. S4C and S4D, respectively).

Overall viability.

Differentiation of HSCs into MKs can be monitored via the expression of the specific MK markers CD41 and CD61. In our *in vitro* model, the percentage of CD41-expressing cells increases over time during differentiation, reaching

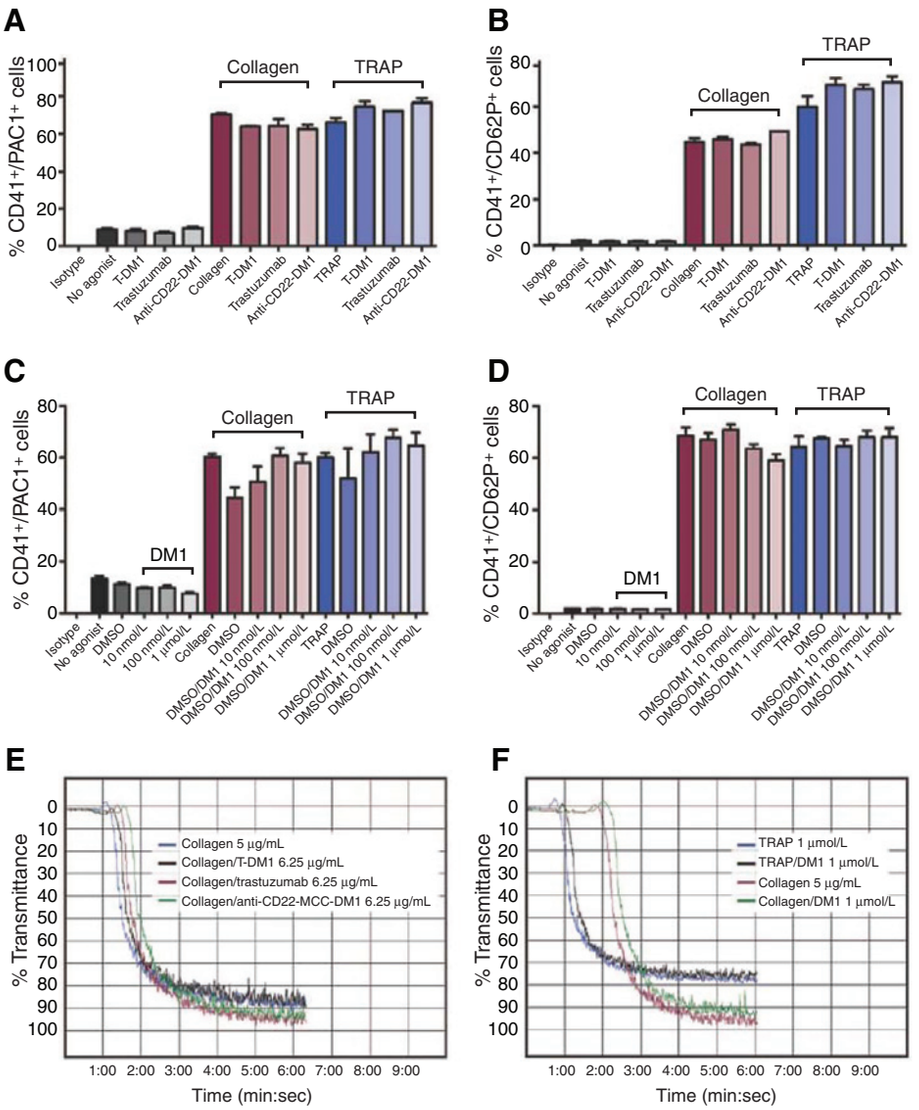

Figure 2.
Neither T-DM1 nor DM1 inhibit agonist-induced platelet activation or aggregation. PRP was incubated with T-DM1, trastuzumab, or anti-CD22-MCC-DM1 followed by collagen or TRAP as described in Materials and Methods. A, PAC1 binding and (B) CD62P expression. (C) PAC1 binding and (D) CD62P expression were assessed in PRP that had been preincubated with various concentrations of DM1 followed by collagen or TRAP. Activation markers were determined by flow cytometry. PRP was preincubated with T-DM1 (E) or DM1 (F) with appropriate controls. Aggregation was induced with collagen or TRAP.

approximately 70% to 90% at day 14, depending on the donor (Supplementary Fig. S1).

We investigated the effect of T-DM1 on HSCs differentiating into MKs and determined the dose–response relationship of this effect (Fig. 3A). T-DM1 appeared to decrease the number of MKs by day 3 with an approximate IC_{50} of 7 μg/mL (∼50 nmol/L). Decreased MK viability after T-DM1 treatment was more pronounced at day 6 with an IC_{50} of approximately 3 μg/mL (∼20 nmol/L), and the IC_{50} remained stable through day 14. Trastuzumab did not decrease MK viability at any dose or time point, whereas the control ADC 5B6-DM1 showed similar viability decreases as T-DM1, suggesting that the T-DM1 effect was due to its DM1 component and not its trastuzumab component.

Viability of immature MKs.

To further investigate the effect of T-DM1 on differentiation of HSCs into MKs, we used flow cytometry to measure total cell number, number of MKs (i.e., $CD41^+/CD61^+$ cells), and cell viability at days 3, 6, 9, and 14 of differentiation (Fig. 3B and D). The number of vehicle- and trastuzumab-treated cells increased over the 14-day time course, reaching a maximal increase of 120-fold over day 0. Continuous exposure of HSCs to DM1 conjugates resulted in a marked decrease relative to vehicle-treated and trastuzumab-treated cells in the percentage of MKs (Fig. 3B). Decreased MK production was observed as early as day 6 (∼50%), and MK numbers decreased further at day 9 (∼90%) and remained at this level at day 14. These changes in MK cell number correlated with a decrease in cell viability (Fig. 3D). These results suggest that decreased cell viability of HSCs differentiating into MKs induced by T-DM1 is mediated by the chemotherapeutic component of T-DM1 (i.e., DM1) and not by the antibody (i.e., trastuzumab).

Viability of maturing MKs.

We conducted similar experiments to determine the effect of T-DM1 on maturing MKs (i.e., days 14–28 of differentiation). By day 28, the number of control- and trastuzumab-treated MKs had increased by approximately 100% compared with day 14 control- and trastuzumab-treated cells (Fig. 3C). As early as day 20, there

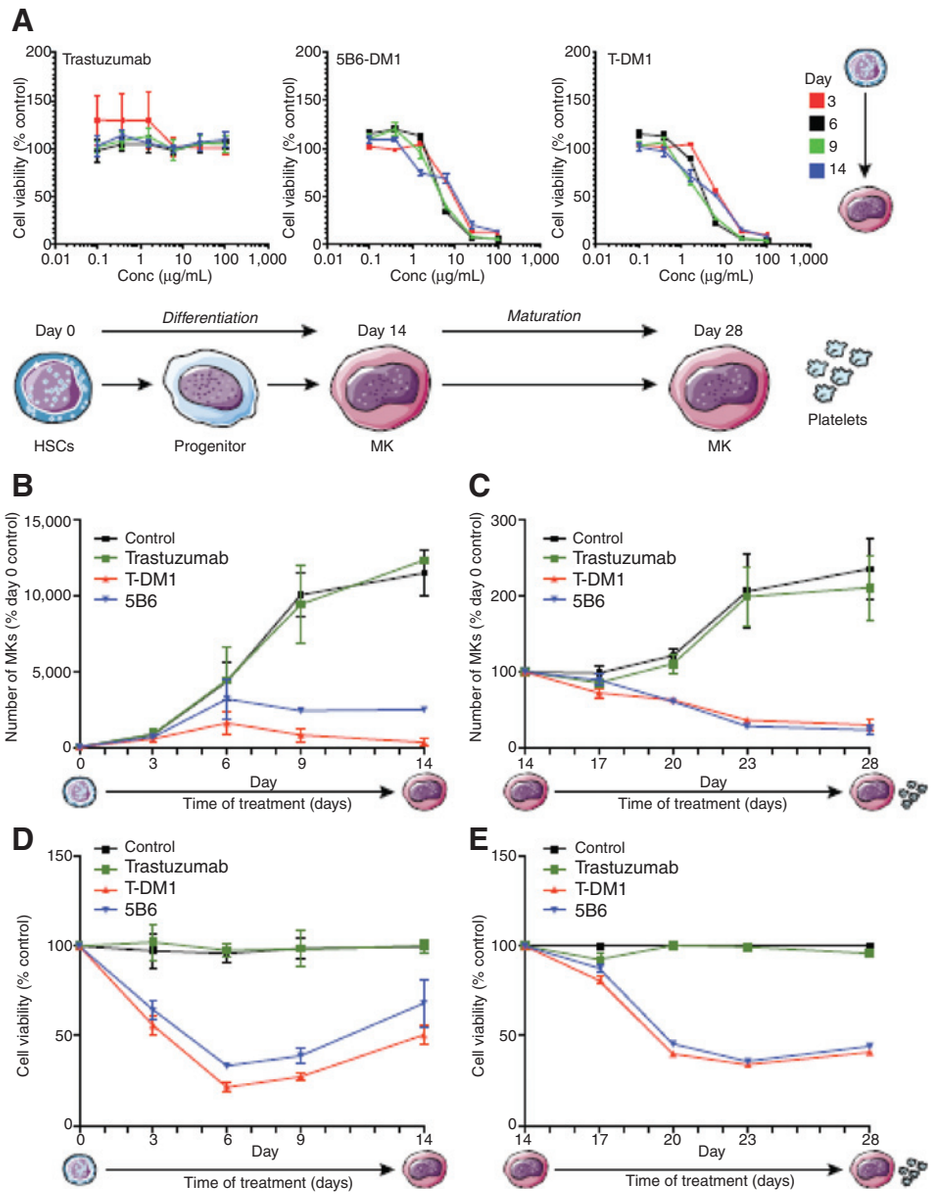

Figure 3.
DM1 conjugates inhibit MK production and viability. HSCs were differentiated into MKs for 14 days and matured for 14 additional days with continuous exposure to the various drugs. A, at day 0, HSCs from two donors were incubated with various concentrations of T-DM1, trastuzumab, or control ADC 5B6-DM1. Cell viability was assessed by flow cytometry at days 3, 6, 9, and 14, and the IC_{50} for each drug was determined. The effect of T-DM1, trastuzumab, and 5B6-DM1 (all at 6.25 μg/mL) on the number of MKs over time during (B) differentiation and (C) maturation was assessed. Flow cytometry was used to quantify MKs using CD41 as a marker. Data are expressed as % day 0 Control (0.23×10^6 MKs at day 0). The effect of T-DM1, trastuzumab, and 5B6-DM1 (all at 6.25 μg/mL) on cell viability over time compared with control during (D) differentiation and (E) maturation was assessed. Average data from two donors are shown.

was an observable reduction in MK cell number (~40%) in the T-DM1– and 5B6-DM1–treated cells. MK numbers decreased further at day 23 (~75%) and remained at this level at day 28 though this decrease in MK cell number was not as great as that seen in differentiating MKs. The decreases in MK cell number correlated with a decrease in cell viability (Fig. 3E).

Taken together, these data suggest that T-DM1 has a cytotoxic effect on both differentiating and maturing MKs that is mediated by its DM1 component and that the effect is more pronounced in differentiating MKs than in maturing MKs.

Effect of T-DM1 on MK ploidy

To further investigate the effect of T-DM1 on MK differentiation from HSCs, we used flow cytometry to evaluate cell ploidy over time (Fig. 4). We observed the expected progression of MK ploidy in the control HSCs over time, with a gradual shift of the cell population from largely 2N at day 4 to a broad population of 64N to 128N cells by day 30. Continuous exposure of developing MKs to DM1-containing ADCs (T-DM1 or 5B6-DM1) arrested the normal progression of megakaryocytopoiesis, as evidenced by inhibition of increased nucleoploidy as early as day 10, resulting in a single broad peak of predominantly 2N to 4N cells by day 30. Unconjugated trastuzumab did not appear to affect megakaryocytopoiesis as trastuzumab-treated HSCs showed a similar nucleoploidy pattern as control-treated cells.

MK uptake and catabolism of T-DM1

To determine whether the reduction in MK number and the arresting of MK development following exposure to T-DM1 were due to the uptake of T-DM1, we assessed the time course of T-[^{3}H]-DM1 uptake in HSCs differentiating into MKs. Uptake of T-DM1 was dependent on the differentiation stage of the cells, with

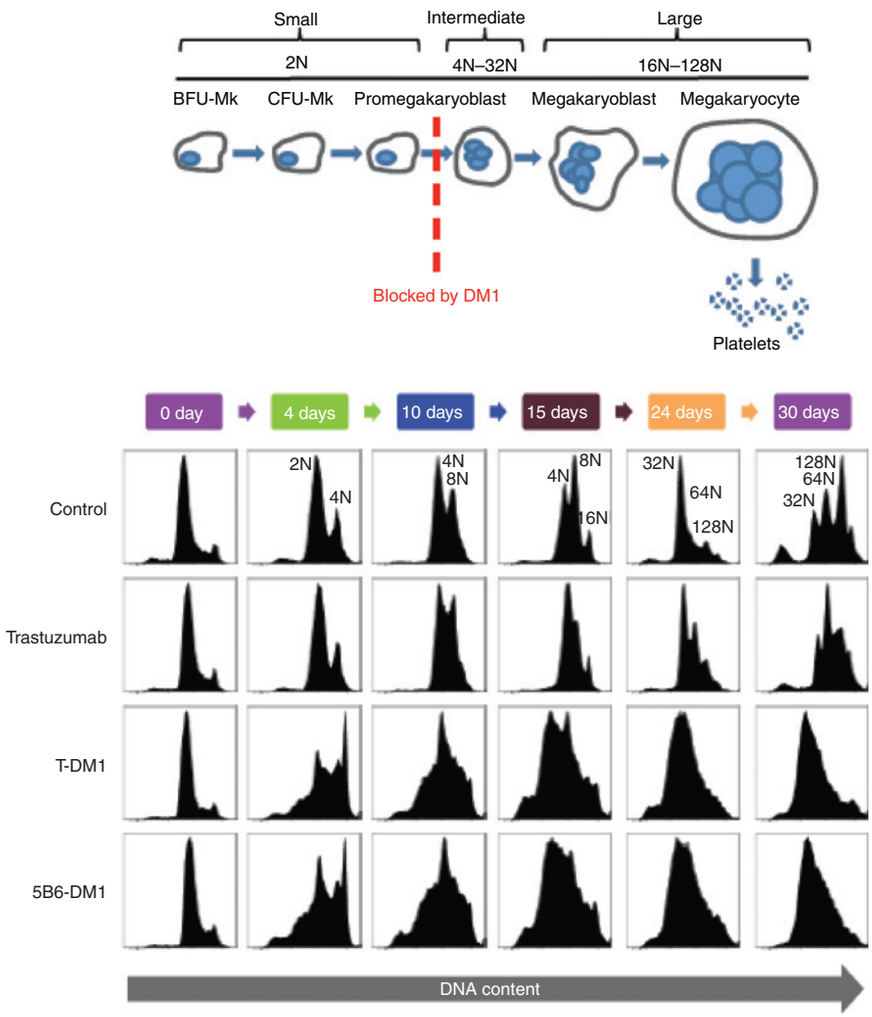

Figure 4.
T-DM1 arrests megakaryocytopoiesis as indicated by ploidy analysis. HSCs were induced to differentiate into MKs in the presence of vehicle control, trastuzumab, T-DM1, or a control ADC 5B6-DM1. Cells were assayed for ploidy by flow cytometry on samples collected daily for 30 days.

the greatest uptake occurring on days 0 through 6 (Supplementary Fig. S5A, protein-bound DM1). The intracellular concentrations of T-DM1 catabolites over time are shown in Table 1. These data are consistent with the viability data demonstrating that precursor MKs (i.e., differentiating MKs) are more sensitive to treatment with DM1-containing antibodies than maturing MKs. In contrast with its pathway in tumor cells (4), T-DM1 was not detectable in lysosomes, as indicated by a lack of costaining of T-DM1 and the lysosomal marker Cy3-LAMP1 (Supplementary Fig. S5B).

To determine whether the uptake of T-DM1 was mediated (completely or in part) through HER2, we first determined whether isolated MK lineage cells (day 14) express HER2. HER2 mRNA was not detected in platelets (Supplementary Fig. S6A) and was detected at only very low levels in $CD61^-$ and $CD61^+$ MKs [0.09 and 0.06, respectively, relative to the housekeeping gene *HP1BP3* (mRNA levels = 1)]. In contrast, MCF-7 breast cancer cells and normal keratinocytes, which are considered to express normal levels of HER2, show HER2 mRNA expression levels of 1.08 and 1.28, respectively, compared with HP1BP3. Furthermore, Western blot analysis of HER2 expression in MK lineage cells ($CD61^+$ and $CD61^-$ populations) and purified platelets (Supplementary Fig. S6B) demonstrated no detectable HER2 protein, indicating that T-DM1 uptake, as well as other effects of T-DM1 on these cells, is not HER2 mediated. These data suggest that the entry of DM1 conjugates into MKs does not occur through HER2 but apparently through binding to FcγRIIa. Trastuzumab, T-DM1, and 5B6-DM1 are all IgG1 isotypes.

To determine whether T-DM1 is internalized by FcγRIIa, fluorescently labeled T-DM1 and trastuzumab were incubated with MKs and evaluated over time. Both T-DM1 (Fig. 5A and C) and trastuzumab (Fig. 5B and C) showed clear binding to the surface of MKs. Flow-cytometric analysis of the surface-bound fluorescent antibodies indicated that maximal binding occurred at 4 hours (Fig. 5C). By 8 hours, the antibodies had been internalized and detection on the cell surface was significantly decreased. When MKs were preincubated with the FcγRII-blocking antibody anti-CD32, surface binding and internalization of both fluorescently labeled T-DM1 (Fig. 5A and C) and trastuzumab (Fig. 5B and C) were markedly decreased (>50%), indicating that FcγRIIa at least partially contributes to the mechanism of T-DM1 and trastuzumab binding and uptake.

To confirm that the uptake of T-DM1 into MKs is HER2 independent and at least partially mediated by FcγRIIa, we evaluated the MK uptake of trastuzumab using two different

Table 1. T-DM1 catabolites quantified in MKs at days 0, 9, and 20

	Concentration (nmol/L)[a,b]		
Time	**DM1[c]**	**MCC-DM1**	**Lys-MCC-DM1**
Day 0, experiment 1[d]	4.03	<LLOQ	<LLOQ
Day 0, experiment 2[d]	4.30	<LLOQ	0.85
Day 9, experiment 1	8.74	<LLOQ	8.18
Day 9, experiment 2	1.57	<LLOQ	1.26
Day 20, experiment 1	3.02	<LLOQ	2.61
Day 20, experiment 2	3.25	<LLOQ	3.45

[a]Processed against appropriate curves; day 20 samples processed against curves from day 9 MKs.
[b]LLOQ for DM1 = 0.488 nmol/L; LLOQ for MCC-DM1 = 1.953 nmol/L; LLOQ for lys-MCC-DM1 = 0.488 nmol/L.
[c]Free DM1 was converted to DM1-NEM for quantification.
[d]Experiments 1 and 2 indicate data from two different donors.

radioprobes, ^{125}I-labeled trastuzumab and ^{111}In-labeled trastuzumab, to mitigate any experimental bias caused by the specific properties of the probe. In general, ^{125}I is rapidly diffusible from cells following intracellular antibody degradation, and therefore the cell-associated ^{125}I represents the kinetics of uptake at that time point, while ^{111}In catabolites tend to accumulate in cells because of properties of the chelator; therefore, the cell-associated ^{111}In represents overall antibody exposure (21). The kinetics of uptake were compared with those of similarly labeled trastuzumab-DANA mutants that lack FcγR binding. At day 0, ^{111}In-trastuzumab-DANA uptake was less than ^{111}In-trastuzumab uptake by 88%, and ^{125}I-trastuzumab-DANA uptake was less than ^{125}I-trastuzumab uptake by 98% (Fig. 5D). Similarly, at day 3, ^{125}I-trastuzumab-DANA uptake was less than ^{125}I-trastuzumab uptake by 99% (Fig. 5E). Both ^{125}I- and ^{111}In-labeled antibodies showed similar trends, indicating that differences in the internalization of the trastuzumab-DANA could not be ascribed to the probe. These data provide further support for an essential role for FcγRIIa in MK uptake of T-DM1.

Effect of T-DM1 on intracellular tubulin and actin microfilaments in maturing MKs

Flow cytometry forward and side scatter analysis suggested that maturing MKs (i.e., days 14 to 28) treated with T-DM1 were larger and more granular than untreated mature MKs (data not shown). To determine whether prolonged T-DM1 exposure has an effect on intracellular microfilament structures, we evaluated the effect of 9 days of T-DM1 exposure on these structures in maturing MKs (i.e., day 14 of differentiation from HSCs). Under control-treated conditions (Supplementary Fig. S7A and S7C), 23-day-old MKs were large and multinucleated, with tubulin and actin clearly delineated. Following prolonged exposure to T-DM1 (Supplementary Fig. S7B and S7D), the microfilament structure had collapsed and appeared diminished and disorganized, suggesting that prolonged exposure to T-DM1 can have a detrimental effect on maturing MKs.

Discussion

Drug-induced thrombocytopenia is relatively common and has been described for hundreds of agents (22). This disorder primarily occurs via two distinct mechanisms: (i) decreased platelet production via cytotoxic effects on MKs and their precursors as observed with some cytotoxic chemotherapeutic agents (23) and (ii) accelerated platelet destruction in peripheral blood via immune-mediated thrombocytopenia (24) and as observed with a number of drug classes including nonsteroidal anti-inflammatories, and sulfonamides (24).

The present study suggests that the thrombocytopenia observed in some T-DM1–treated patients is not immune mediated and may result from decreased platelet production, which is consistent with inhibition of MK differentiation, with no direct functional effect on platelets. The most pronounced effects of T-DM1 appear to occur during the differentiation process from HSCs to MKs. Our data show that trastuzumab, T-DM1, and a control DM1-containing ADC were all internalized by MKs and that HER2 was not expressed on MKs or platelets. Internalization could be inhibited by either blockade of the interaction between FcγRIIa using anti-CD32 or by using the Fc-mutant trastuzumab-DANA, which is unable to bind FcγR. Furthermore, the observed effect on MKs occurred with T-DM1 and the control DM1-containing ADC, but not with trastuzumab. These data support the hypothesis that the effects on MK formation are mediated by the DM1 component of T-DM1 but require an interaction of the Fc domain of T-DM1 with FcγRIIa for internalization. The mechanism of release of the DM1 moiety from the internalized complex is at present unknown, as we could not detect colocalization of the internalized antibody with lysosomal LAMP1 by immunofluorescence.

Our data are consistent with a previous report which found—using different methods—that T-DM1–induced platelet decreases by decreasing platelet production via an effect on the cytoskeleton of differentiating MKs (13). The proposed mechanism of decreased platelet production (i.e., cytoskeletal disruption in differentiating MKs) is also consistent with our data, showing cytoskeletal disorganization in maturing MKs when they were subjected to prolonged T-DM1 exposure (Supplementary Fig. S7B and S7D). We also show effects in earlier stages of differentiation and speculate that this occurs via a similar mechanism. Our data differ from those reported by Thon and colleagues in that these investigators concluded that T-DM1–induced thrombocytopenia occurs via a mechanism that is both HER2 and FcγRIIa independent, based on the controls used and due to the fact that mouse MKs and platelets do not express FcγRIIa (25). Our data clearly demonstrate an FcγRIIa-dependent mechanism of internalization of T-DM1 in human MKs. Differences between the results found in the two studies could be attributed partly to differences in experimental methodologies and species differences.

T-DM1–mediated effects appeared to be more pronounced in differentiating MKs (i.e., day 0–14 cells) than in maturing MKs (day 14–28 cells). Differentiating MKs bound, internalized, and catabolized T-DM1 to a much greater degree than maturing MKs. However, T-DM1 did have an effect on maturing MKs as noted, above. T-DM1 exposure resulted in decreased cell viability (but to a lesser extent than that seen in differentiating MKs) and induced disruption of the cytoskeletal structure in these cells.

The mechanisms of T-DM1–induced thrombocytopenia described here are consistent with the pattern of cyclic decline and rebound of platelet levels seen during treatment with T-DM1 (7, 10). In most patients receiving T-DM1, platelet levels show an acute drop and reach a nadir during cycle 1 and return to baseline levels between doses (6, 7, 9, 10). Some patients do exhibit a slow drift downward in platelet counts with repeated cycles of T-DM1, resembling the pattern induced by cumulative myelosuppression seen with other cytotoxic agents (10). However, even in those patients with a slow downward shift in platelet levels over subsequent cycles, platelet counts tend to stabilize at a level less severe than grade 3 thrombocytopenia (10). Indeed, grade 3 or

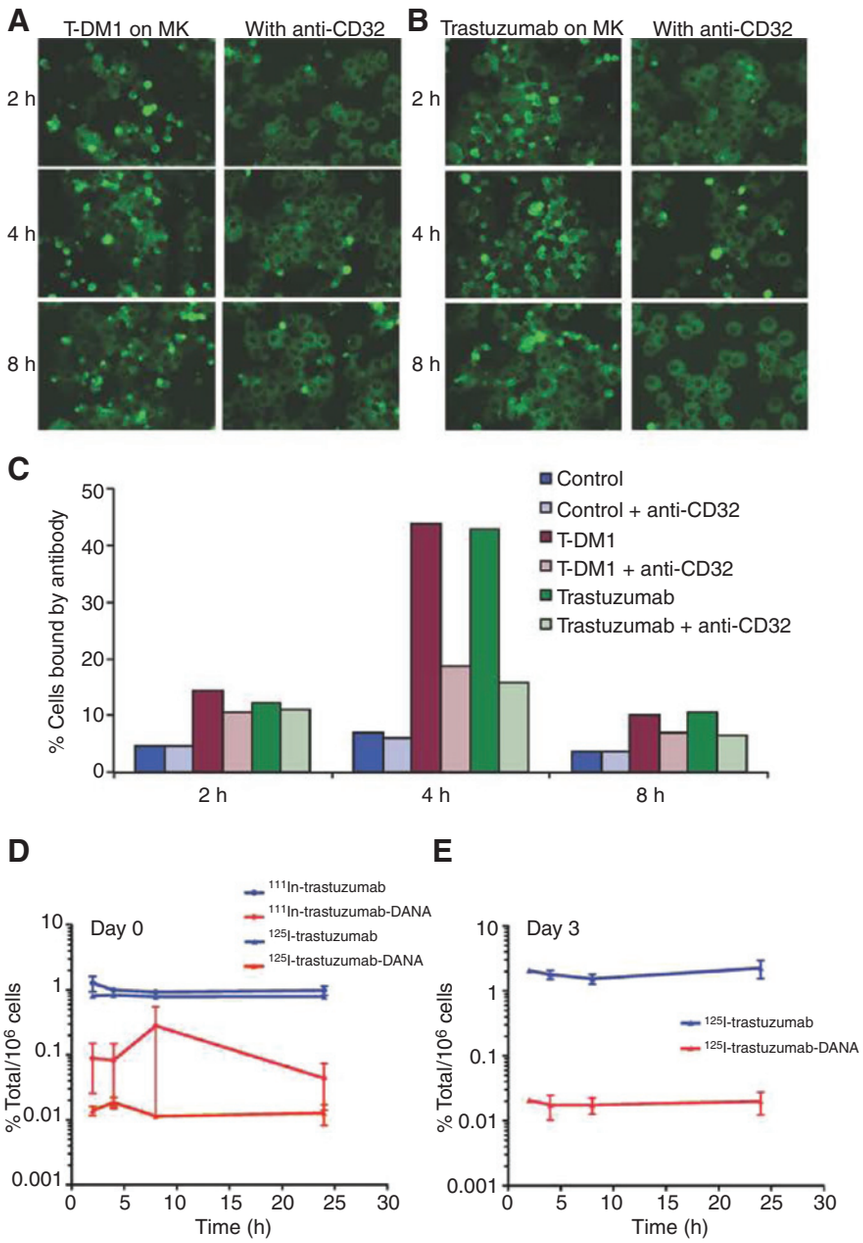

Figure 5.
FcγRIIa mediates T-DM1 internalization. Fluorescently conjugated (A) T-DM1 and (B) trastuzumab are internalized by MKs (differentiated from HSCs for 14 days; panels 1–3). Preincubation with the FcRγII–blocking antibody anti-CD32 results in a marked decrease in fluorescently labeled T-DM1 (A, panels 4–6) and trastuzumab (B, panels 4–6) with greater surface localization. C, quantification of surface binding of T-DM1 and trastuzumab, as assessed by flow cytometry. D, uptake of ^{111}In-trastuzumab, ^{111}In-trastuzumab-DANA, ^{125}I-trastuzumab, and ^{125}I-trastuzumab-DANA in HSCs at day 0 of differentiation as indicated by total counts per minute. E, ^{125}I-trastuzumab and ^{125}I-trastuzumab-DANA in HSCs at day 3 of differentiation as indicated by total counts per minute. Error bars indicate SD.

higher thrombocytopenia occurred in only 4.7% to 12.9% of patients in the phase III studies with T-DM1 (6, 8). The kinetics of thrombocytopenia seen during treatment suggest that T-DM1 affects a specific platelet precursor pool. We further hypothesize that depletion of this pool results in either a shift in the equilibrium in the bone marrow to generate more platelet precursor cells to manage the platelet depletion (26) or that a new lineage that is less sensitive to T-DM1 becomes dominant and platelet counts stabilize (10), or both. This hypothesis is consistent with our *in vitro* studies that show a profound effect on platelet precursors (proliferating MKs).

In phase III studies of T-DM1, other severe hematologic toxicities occurred with much lower frequency than thrombocytopenia. Grade ≥3 anemia occurred in 2.7% of patients, grade ≥3 neutropenia occurred in 2.0% to 2.5%, and grade ≥3 leucopenia occurred in <2% of patients (6, 8). These clinical data are consistent with an FcγRIIa-dependent mechanism because FcγRIIa is expressed at relatively low (or absent) levels in CD34$^+$ cells isolated from human cord blood (27) and in lymphocyte lineages in normal human bone marrow (28). However CD32 is expressed in myeloid lineages (28). It is interesting to speculate that the small fraction of patients who exhibit a slow downward drift in platelet counts over time may indeed have a polymorphism(s) in FcγRIIa or a different pattern of FcγRIIa expression which renders their MKs and/or other hematologic lineage precursors (myeloid) more susceptible to T-DM1. Additional studies to evaluate biomarkers (such as FcR polymorphisms) associated with increased susceptibility to T-DM1–induced thrombocytopenia are underway to further characterize the mechanism of T-DM1–induced thrombocytopenia.

The cyclical pattern of platelet counts over time seen in clinical studies may be explained by the interaction between T-DM1 and FcγRIIa. The affinity of human IgG1 for FcγRIIa is 0.85 to 0.90 μmol/L (29). At the established clinical dose of 3.6 mg/kg q3w, the observed C_{max} of T-DM1 is 83.4 μg/mL (30). At this concentration, the occupancy of FcγRIIa would be expected to be approximately 35%. We postulate that binding of T-DM1, near or at its C_{max}, to FcγRIIa drives sufficient transient internalization and subsequent degradation of the conjugate to release DM1. This in turn impairs the proliferation and differentiation of proplatelet precursor(s), which temporarily depletes this species from contributing to platelet production. The transient nature of the binding, internalization, and degradation process may then explain the transient and reversible nature of the thrombocytopenia observed in patients treated with T-DM1.

Taken together, these data support the hypothesis that the thrombocytopenia observed in clinical trials with T-DM1 is mediated in large part by impaired platelet production from MKs within the bone marrow. We further hypothesize that other ADCs with an IgG1 backbone conjugated to a tubulin inhibitor via an MCC linker could potentially result in a clinical risk for dose-limiting thrombocytopenia.

Disclosure of Potential Conflicts of Interest

H. Uppal is an employee of Medivation Inc. G.D. Lewis Phillips is an employee of Genentech. M.X. Sliwkowski holds ownership interest (including patents) in Roche. No potential conflicts of interest were disclosed by the other authors.

Authors' Contributions

Conception and design: H. Uppal, K. Mahapatra, O. Saad, S. Olsen, D. Hartley, M.X. Sliwkowski, S. Girish, V. Ramakrishnan

Development of methodology: H. Uppal, E. Doudement, K. Mahapatra, W.C. Darbonne, D. Bumbaca, X.-Y. Du, K. Bowles, G.D. Lewis Phlliips, V. Ramakrishnan

Acquisition of data (provided animals, acquired and managed patients, provided facilities, etc.): H. Uppal, E. Doudement, K. Mahapatra, W.C. Darbonne, D. Bumbaca, B.-Q. Shen, X.-Y. Du, O. Saad, G.D. Lewis Phlliips, D. Hartley, V. Ramakrishnan

Analysis and interpretation of data (e.g., statistical analysis, biostatistics, computational analysis): H. Uppal, E. Doudement, K. Mahapatra, W.C. Darbonne, D. Bumbaca, B.-Q. Shen, X.-Y. Du, O. Saad, S. Olsen, G.D. Lewis Phlliips, D. Hartley, M.X. Sliwkowski, S. Girish, V. Ramakrishnan

Writing, review, and/or revision of the manuscript: H. Uppal, E. Doudement, K. Mahapatra, W.C. Darbonne, D. Bumbaca, B.-Q. Shen, O. Saad, S. Olsen, G.D. Lewis Phlliips, D. Hartley, M.X. Sliwkowski, S. Girish, D. Dambach, V. Ramakrishnan

Administrative, technical, or material support (i.e., reporting or organizing data, constructing databases): H. Uppal, K. Mahapatra, W.C. Darbonne, D. Hartley, V. Ramakrishnan

Study supervision: H. Uppal, K. Mahapatra, B.-Q. Shen, D. Hartley, V. Ramakrishnan

Other (conduct of experiments): H. Uppal

Other [designed and implemented the flow cytometry and imaging panels across multiple human bone marrow donors (for statistical significance) to study the mechanism of thrombocytopenia upon treatment with TDM1]: K. Mahapatra

Acknowledgments

The authors thank Jay Tibbitts, Jun Guo, Guangmin Li, and Neelima Koppada.

Grant Support

This work was supported by Genentech Inc. Support for third-party writing assistance, furnished by Holly Strausbaugh, was provided by Genentech, Inc.

The costs of publication of this article were defrayed in part by the payment of page charges. This article must therefore be hereby marked *advertisement* in accordance with 18 U.S.C. Section 1734 solely to indicate this fact.

Received August 12, 2014; revised October 9, 2014; accepted October 13, 2014; published OnlineFirst November 4, 2014.

References

1. Chari RV. Targeted cancer therapy: conferring specificity to cytotoxic drugs. Acc Chem Res 2008;41:98–107.
2. Lewis Phillips GD, Li G, Dugger DL, Crocker LM, Parsons KL, Mai E, et al. Targeting HER2-positive breast cancer with trastuzumab-DM1, an antibody-cytotoxic drug conjugate. Cancer Res 2008;68:9280–90.
3. Junttila TT, Li G, Parsons K, Phillips GL, Sliwkowski MX. Trastuzumab-DM1 (T-DM1) retains all the mechanisms of action of trastuzumab and efficiently inhibits growth of lapatinib insensitive breast cancer. Breast Cancer Res Treat 2011;128:347–56.
4. Erickson HK, Lewis Phillips GD, Leipold DD, Provenzano CA, Mai E, Johnson HA, et al. The effect of different linkers on target cell catabolism and pharmacokinetics/pharmacodynamics of trastuzumab maytansinoid conjugates. Mol Cancer Ther 2012;11:1133–42.
5. Hurvitz SA, Dirix L, Kocsis J, Bianchi GV, Lu J, Vinholes J, et al. Phase II randomized study of trastuzumab emtansine versus trastuzumab plus docetaxel in patients with human epidermal growth factor receptor 2-positive metastatic breast cancer. J Clin Oncol 2013;31:1157–63.
6. Verma S, Miles D, Gianni L, Krop IE, Welslau M, Baselga J, et al. EMILIA Study Group. Trastuzumab emtansine for HER2-positive advanced breast cancer. N Engl J Med 2012;367:1783–91.
7. Krop IE, LoRusso P, Miller KD, Modi S, Yardley D, Rodriguez G, et al. A phase II study of trastuzumab emtansine in patients with human epidermal growth factor receptor 2-positive metastatic breast cancer who were previously treated with trastuzumab, lapatinib, an anthracycline, a taxane, and capecitabine. J Clin Oncol 2012;30:3234–41.
8. Krop IE, Kim SB, González-Martín A, LoRusso PM, Ferrero JM, Smitt M, et al. TH3RESA study collaborators. Trastuzumab emtansine versus treatment of physician's choice for pretreated HER2-positive advanced breast cancer (TH3RESA): a randomized, open-label, phase 3 trial. Lancet Oncol 2014;15:689–99.
9. Krop IE, Beeram M, Modi S, Jones SF, Holden SN, Yu W, et al. Phase I study of trastuzumab-DM1, an HER2 antibody-drug conjugate, given every 3 weeks to patients with HER2-positive metastatic breast cancer. J Clin Oncol 2010;28:2698–704.
10. Bender BC, Schaedeli-Stark F, Koch R, Joshi A, Chu YW, Rugo H, et al. A population pharmacokinetic/pharmacodynamic model of thrombocytopenia characterizing the effect of trastuzumab emtansine (T-DM1) on platelet counts in patients with HER2-positive metastatic breast cancer. Cancer Chemother Pharmacol 2012;70:591–601.
11. Bühring HJ, Sures I, Jallal B, Weiss FU, Busch FW, Ludwig WD, et al. The receptor tyrosine kinase p185HER2 is expressed on a subset of B-lymphoid blasts from patients with acute lymphoblastic leukemia and chronic myelogenous leukemia. Blood 1995;86:1916–23.
12. Ramakrishnan V, Reeves PS, DeGuzman F, Deshpande U, Ministri-Madrid K, DuBridge RB, et al. Increased thrombin responsiveness in platelets from mice lacking glycoprotein V. Proc Natl Acad Sci U S A 1999;96:13336–41.
13. Thon JN, Devine MT, Jurak Begonja A, Tibbitts J, Italiano JE Jr. High-content live cell imaging assay used to establish mechanism of trastuzumab emtansine (T-DM1)-mediated inhibition of platelet production. Blood 2012;120:1975–84.
14. Wu Z, Markovic B, Chesterman CN, Chong BH. Characterization of Fc gamma receptors on human megakaryocytes. Thromb Haemost 1996;75:661–7.
15. Boylan B, Gao C, Rathore V, Gill JC, Newman DK, Newman PJ. Identification of FcgammaRIIa as the ITAM-bearing receptor mediating

alphaIIbbeta3 outside-in integrin signaling in human platelets. Blood 2008;112:2780–6.
16. Shields RL, Namenuk AK, Hong K, Meng YG, Rae J, Briggs J, et al. High resolution mapping of the binding site on human IgG1 for Fc gamma RI, Fc gamma RII, Fc gamma RIII, and FcRn and design of IgG1 variants with improved binding to the Fc gamma R. J Biol Chem 2001;276: 6591–604.
17. Chizzonite R, Truitt T, Podlaski FJ, Wolitzky AG, Quinn PM, Nunes P, et al. IL-12: monoclonal antibodies specific for the 40-kDa subunit block receptor binding and biologic activity on activated human lymphoblasts. J Immunol 1991;147:1548–56.
18. Sosabowski JK, Mather SJ. Conjugation of DOTA-like chelating agents to peptides and radiolabeling with trivalent metallic isotopes. Nat Protoc 2006;1:972–6.
19. Girish S, Gupta M, Wang B, Lu D, Krop IE, Vogel CL, et al. Clinical pharmacology of trastuzumab emtansine (T-DM1): an antibody-drug conjugate in development for the treatment of HER2-positive cancer. Cancer Chemother Pharmacol 2012;69:1229–40.
20. Josefsson EC, James C, Henley KJ, Debrincat MA, Rogers KL, Dowling MR, et al. Megakaryocytes possess a functional intrinsic apoptosis pathway that must be restrained to survive and produce platelets. J Exp Med 2011;208:2017–31.
21. Boswell CA, Bumbaca D, Fielder PJ, Khawli LA. Compartmental tissue distribution of antibody therapeutics: experimental approaches and interpretations. AAPS J 2012;14:612–8.
22. Visentin GP, Liu CY. Drug-induced thrombocytopenia. Hematol Oncol Clin North Am 2007;21:685–96.
23. Zeuner A, Signore M, Martinetti D, Bartucci M, Peschle C, De Maria R. Chemotherapy-induced thrombocytopenia derives from the selective death of megakaryocyte progenitors and can be rescued by stem cell factor. Cancer Res 2007;67:4767–73.
24. van den Bemt PM, Meyboom RHB, Egberts AC. Drug-induced immune thrombocytopenia. Drug Saf 2004;27:1243–52.
25. Zhi H, Rauova L, Hayes V, Gao C, Boylan B, Newman DK, et al. Cooperative integrin/ITAM signaling in platelets enhances thrombus formation *in vitro* and *in vivo*. Blood 2013;121:1858–67.
26. Hunt P, Zsebo KM, Hokom MM, Hornkohl A, Birkett NC, del Castillo JC, et al. Evidence that stem cell factor is involved in the rebound thrombocytosis that follows 5-fluorouracil treatment. Blood 1992;80: 904–11.
27. Yoo ES, Ryu KH, Park HY, Seong CM, Chung WS, Kim SC, et al. Myeloid differentiation of human cord blood CD34+ cells during ex vivo expansion using thrombopoietin, flt3-ligand and/or granulocyte-colony stimulating factor. Br J Haematol 1999;105:1034–40.
28. Saito Y, Kitamura H, Hijikata A, Tomizawa-Murasawa M, Tanaka S, Takagi S, et al. Identification of therapeutic targets for quiescent, chemotherapy-resistant human leukemia stem cells. Sci Transl Med 2010;2:17ra9.
29. Richards JO, Karki S, Lazar GA, Chen H, Dang W, Desjarlais JR. Optimization of antibody binding to FcgammaRIIa enhances macrophage phagocytosis of tumor cells. Mol Cancer Ther 2008;7:2517–27.
30. Girish S, Li C. Clinical Pharmacology and assay considerations for characterizing pharmacokinetics and understanding efficacy and safety of ADCs. Future Science Ltd; 2014.